Note: Improved line strengths of rovibrational and rotational transitions within the $X^3\Sigma^-$ ground state of NH

James S. A. Brooke,[1,a)] Peter F. Bernath,[1,2] and Colin M. Western[3]
[1]*Department of Chemistry, University of York, York YO10 5DD, United Kingdom*
[2]*Department of Chemistry and Biochemistry, Old Dominion University, 4541 Hampton Boulevard, Norfolk, Virginia 23529-0126, USA*
[3]*School of Chemistry, University of Bristol, Cantock's Close, Bristol BS8 1TS, United Kingdom*

(Received 16 April 2015; accepted 23 June 2015; published online 13 July 2015)

[http://dx.doi.org/10.1063/1.4923422]

We recently published line lists, including positions and transition strengths, for the NH $X^3\Sigma^-$ state rovibrational and rotational transitions.[1] The calculation of the transition strengths involved an approximation, but the method has since been improved (in our OH $^2\Pi$ work[2]) and this approximation removed, resulting in a more accurate distribution of intensity between different spin-component transitions. The previously published NH transition strengths are already in use, and as a single adjustment to the calculations can result in an improvement in the transition strengths, we believe that an updated list should be provided.

NH is an important molecule in astronomy, as its transitions have been used to calculate the N abundance in the Sun[3,4] and other stars,[5–8] and it has also been detected in comets[9] and diffuse interstellar clouds.[10–13] Other areas in which its transitions are useful are those of combustion science[14,15] and magnetic trapping,[16–23] which has applications to fields such as quantum computing[24] and high precision spectroscopy.[25,26] Use of the previous line list could result in slightly inaccurate NH and N abundances being obtained in astronomical and combustion environments, and we would like to direct potential users to the updated list presented in this note.

The calculation method will briefly be described here, but for a full description, see Refs. 1 and 27. Molecular constants are obtained from fits to available experimental line positions, and equilibrium constants are determined from fits to the molecular constants G_v and B_v. A potential energy curve (PEC) is calculated using the program RKR1,[28] which takes the equilibrium constants as input. The PEC and dipole moment function (DMF) (from Refs. 18 and 1) are then entered along with a dissociation energy (DE) into the program LEVEL.[29] The DE used is 27 176 ± 280 cm^{-1} from the theoretical calculations of Espinosa-García *et al.*[30] This compares well with a range of experimental values that they reported (26 535.91–27 987.396 cm^{-1} (Refs. 31–33)), and with another theoretical value of 27 181 ± 242 cm^{-1}.[34] LEVEL extrapolates the PEC (using the DE as a limit) and calculates vibrational wavefunctions and then transition matrix elements (MEs) between the relevant states. These MEs include the Herman Wallis (H-W) effect (vibration-rotation interaction). Finally, PGOPHER[35] takes the molecular constants and MEs as input, and calculates transition strengths as Einstein *A* values.

LEVEL does not include electron spin, and its MEs are in terms of *N* and not *J*, and we describe these as Hund's case (b) MEs. The calculations in PGOPHER use a case (a) basis, and so the MEs from LEVEL need to be converted from case (b) to (a) before entry into PGOPHER. A transformation equation (TE) to perform this conversion was derived in Ref. 27, with the full derivation in the Appendix to that paper.

The TE was revisited in more recent work on the $X^2\Pi$ state of OH, where it was found that the transformation of the vibronic transition moment to the case (a) basis introduced small $\Delta\Sigma \neq 0$ MEs. This is unexpected for an electric dipole transition and is a consequence of the *N* dependence of the vibronic transition dipole. As shown in Ref. 2, if the dipole is independent of *N* (i.e., no H-W effect), the $\Delta\Sigma \neq 0$ MEs are zero as expected for Hund's case (a). Note that this effect is distinct from the standard Hund's case (a)/case (b) mixing, which is already accounted for. The revised TE is

$$\begin{aligned}\langle \eta'\Lambda'; S\Sigma'|T^k_{\Omega'-\Omega}(\mu, J'\Omega' J\Omega)|\eta\Lambda; S\Sigma\rangle &= (-1)^{J'-\Omega'}\begin{pmatrix} J' & k & J \\ -\Omega' & \Omega'-\Omega & \Omega\end{pmatrix}^{-1} \\ &\times \sum_{N,N'}(-1)^{N'-N+\Omega'-\Omega+S+J+\Lambda'+k}(2N'+1)(2N+1) \\ &\times \begin{pmatrix} J' & S & N' \\ \Omega' & -\Sigma' & -\Lambda'\end{pmatrix}\begin{pmatrix} J & S & N \\ \Omega & -\Sigma & -\Lambda\end{pmatrix}\begin{Bmatrix} N' & J' & S \\ J & N & k\end{Bmatrix} \\ &\times \begin{pmatrix} N' & k & N \\ -\Lambda' & \Lambda'-\Lambda & \Lambda\end{pmatrix}\langle \eta'\Lambda'|T^k_{\Lambda'-\Lambda}(\mu, N'N)|\eta\Lambda\rangle, \quad (1)\end{aligned}$$

where η represents the remaining electronic and vibrational quantum numbers, *k* is the rank of the tensor (equal to 1 for single photon transitions), and $T^k_{\Omega'-\Omega}(\mu, J'\Omega' J\Omega)$ and $T^k_{\Lambda'-\Lambda}(\mu, N'N)$ are the molecule fixed electric dipole operators in spherical tensor notation. For a more detailed description of the changes to the TE, see our recent OH work.[2] The effect of the change is that small $\Delta\Sigma \neq 0$ MEs appear in the Hund's case (a) transition matrices. For example, for the (1,0) R(4) transition, the case (a) symmetrized transition matrix set up by PGOPHER when the old version of the TE is used is that in the left panel of Table I. This matrix is then combined in PGOPHER with the eigenvectors resulting from the diagonal-

a)jsabrooke@gmail.com. Now at School of Chemistry, University of Leeds, United Kingdom.

TABLE I. Transition matrices for the (1,0), R(4) transition, when the old transformation equation (TE) is used. Left: *e* parity matrix, right: transformed matrix in terms of the real states. All values are in debye.

	$J'=5$ $\Sigma=\pm1$	$J'=5$ $\Sigma=0$		$J'=5$ F_{1e}	$J'=5$ F_{3e}
$J=4$ $\Sigma=\pm1$	−0.148 372	0	$J=4$ F_{1e}	−0.149 797	0.000 122
$J=4$ $\Sigma=0$	0	−0.151 539	$J=4$ F_{3e}	0.003 031	−0.150 099

ization of the Hamiltonian matrices to produce the MEs in terms of the real states, as shown in the right panel of the table. Only the *e* parity matrix is shown, as the *f* parity matrix consists of only one element ($\Sigma = \pm1$) and is unaffected by the change in the TE as there are no $\Delta\Sigma \neq 0$ MEs. When the adjusted TE is used, the off-diagonal MEs appear as in the left panel of Table II, and the final MEs are those in the right panel.

The calculations have been performed using the same molecular constants, PEC, DMF, and methods as in the previous work, but with use of the adjusted TE to convert the transition MEs from case (b) to (a).

The updated line list contains all possible transitions with v′ and v″ up to 6, and J up to between 25 and 44, depending on the band. The vibrational band $A_{v'v}$ and $f_{v'v}$ values have also been updated. $A_{v'v}$ values are equal to the sum of $A_{J'J}$ values for transitions between v′ and v, with $J' = 1$ (an average of the three F' values is taken).[36] $f_{v'v}$ values were then calculated using the same method as in the previous work.[1] The line list, molecular constants, *ab initio* DMF, PEC, $A_{v'v}$ and $f_{v'v}$ values, and PGOPHER input file (which contains all transition MEs) are available in the supplementary material.[37]

The H-W effect causes the R branches to be much stronger than the P branches, and the ratio of R branch to P branch intensity for the same upper N level (H-W ratio) varies with N. As these ratios use the same upper N levels (for comparison with an emission spectrum), the effects of level population are canceled, and so they are useful for the comparison of observed and calculated intensity ratios.

Each N'-N transition is mainly made up of three fine structure J'-J transitions, with $F' = F''$. The main effect of the inclusion of $\Delta\Sigma \neq 0$ MEs on a particular N'-N transition is a small redistribution of intensity between the possible J'-J transitions. The observed spectrum was not of high enough resolution to resolve the fine structure adequately for intensity measurements, and instead the sum of the fine structure transitions was used to calculate observed H-W ratios. The redistribution of intensity therefore has little effect on the calculated ratios, so unlike in our OH work, we cannot offer any experimental validation of the updated transformation, though the agreement with the sum remains good.

TABLE II. Same as Table I, but when the new TE is used.

	$J'=5$ $\Sigma=\pm1$	$J'=5$ $\Sigma=0$		$J'=5$ F_{1e}	$J'=5$ F_{3e}
$J=4$ $\Sigma=\pm1$	−0.148 372	0.004 912	$J=4$ F_{1e}	−0.144 421	0.000 099 2
$J=4$ $\Sigma=0$	0.005 897	−0.151 539	$J=4$ F_{3e}	0.002 024	−0.155 484

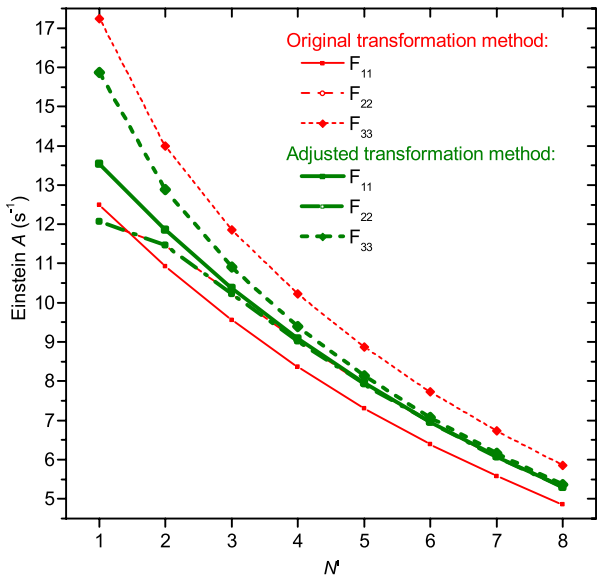

FIG. 1. Einstein A values for the three strong components of the (1,0) band P branch with the two different TEs. A single curve shows for the F_{22} transitions, as they are not affected by the type of transformation.

Figure 1 shows the change in transition strengths resulting from the change in the TE, using the (1,0) band as an example. The general trend is that transitions with the same N value now have a smaller range of A values than they did with the original TE. The A values become closer with increasing N, so that by $N' = 8$ they are almost identical. Despite this, the lines within a triplet in the spectrum will still have noticeably different strengths, as the levels involved have different values of J, and therefore different degeneracies.

For the pure rotational transitions, the effect of the adjusted TE is less than for the rovibrational transitions. At low N, the A values are very similar for both equations, though they diverge slightly with increasing N.

The change in Einstein A generally increases with decreasing transition strength, with a maximum change of about six orders of magnitude. The large changes only occur for transitions that are so weak that they are unlikely to ever be observed, most of which are high Δv or satellite transitions. The largest change for any transition that has previously been observed is about 18%, with most below 4%.

It has been shown that it is possible to improve part of the method used to calculate a previous NH $X^3\Sigma^-$ line list of positions and transition strengths. The calculations have been repeated, and an updated line list has been provided in the supplementary material.[37] This will be useful in fields such as astronomy, combustion science, and magnetic trapping, and will enable the calculation of more accurate NH and nitrogen abundances compared to the previous list.

Support for this work was provided by a Research Project Grant from the Leverhulme Trust and a Department of Chemistry (University of York) studentship.

[1]J. S. A. Brooke *et al.*, J. Chem. Phys. **141**, 054310 (2014).
[2]J. S. A. Brooke *et al.*, "Line strengths of rovibrational and rotational transitions within the $X^2\Pi$ ground state of OH," J. Quant. Spectrosc. Radiat. Transfer (submitted).
[3]N. Grevesse *et al.*, Astron. Astrophys. **232**, 225 (1990).
[4]M. Asplund *et al.*, Annu. Rev. Astron. Astrophys. **47**, 481 (2009).
[5]D. L. Lambert *et al.*, Astrophys. J. **284**, 223 (1984).
[6]D. L. Lambert *et al.*, Astrophys. J., Suppl. Ser. **62**, 373 (1986).
[7]V. V. Smith and D. L. Lambert, Astrophys. J. **311**, 843 (1986).
[8]W. Aoki and T. Tsuji, Astron. Astrophys. **328**, 175 (1997).
[9]M. M. Litvak and E. N. R. Kuiper, Astrophys. J. **253**, 622 (1982).
[10]D. M. Meyer and K. C. Roth, Astrophys. J. Lett. **376**, L49 (1991).
[11]I. A. Crawford and D. A. Williams, Mon. Not. R. Astron. Soc. **291**, L53 (1997).
[12]J. R. Goicoechea *et al.*, Astrophys. J. **600**, 214 (2004).
[13]T. Weselak *et al.*, Mon. Not. R. Astron. Soc. **400**, 392 (2009).
[14]J. A. Miller and C. T. Bowman, Prog. Energy Combust. Sci. **15**, 287 (1989).
[15]L. D. Smoot *et al.*, Prog. Energy Combust. Sci. **24**, 385 (1998).
[16]W. C. Campbell *et al.*, Phys. Rev. Lett. **98**, 213001 (2007).
[17]S. Hoekstra *et al.*, Phys. Rev. A **76**, 063408 (2007).
[18]W. C. Campbell *et al.*, Phys. Rev. Lett. **100** (2008).
[19]M. T. Hummon *et al.*, Phys. Rev. A **78**, 050702 (2008).
[20]M. Kajita, Phys. Rev. A **74**, 032710 (2006).
[21]L. M. C. Janssen *et al.*, Phys. Rev. A **83**, 022713 (2011).
[22]L. M. C. Janssen *et al.*, J. Chem. Phys. **134**, 124309 (2011).
[23]L. M. C. Janssen *et al.*, Eur. Phys. J. D **65**, 177 (2011).
[24]D. Demille, Phys. Rev. Lett. **88**, 067901 (2002).
[25]M. Kajita, Phys. Rev. A **74**, 035403 (2006).
[26]H. L. Bethlem and W. Ubachs, Faraday Discuss. **142**, 25 (2009).
[27]J. S. A. Brooke *et al.*, Astrophys. J., Suppl. Ser. **210**, 23 (2014).
[28]R. J. Le Roy, University of Waterloo Chemical Physics Research Report (University of Waterloo, 2004), http://scienide2.uwaterloo.ca/~rleroy/rkr/.
[29]R. J. Le Roy, University of Waterloo Chemical Physics Research Report (University of Waterloo, 2007), http://scienide2.uwaterloo.ca/~rleroy/level/.
[30]J. Espinosa-García *et al.*, Chem. Phys. Lett. **233**, 220 (1995).
[31]W. R. M. Graham and H. Lew, Can. J. Phys. **56**, 85 (1978).
[32]K. P. Huber and G. Herzberg, "Molecular spectra and molecular structure. Volume IV: Constants of diatomic molecules," in *Molecular Spectra and Molecular Structure* (Van Nostrand Reinhold, 1979).
[33]A. Hofzumahaus and F. Stuhl, J. Chem. Phys. **82**, 5519 (1985).
[34]C. W. Bauschlicher, Jr. and S. R. Langhoff, Chem. Phys. Lett. **135**, 67 (1987).
[35]C. M. Western, PGOPHER, a program for simulating rotational structure (v. 7.1.293), 2014.
[36]P. F. Bernath, *Spectra of Atoms and Molecules*, 3rd ed. (Oxford University Press, 2015).
[37]See supplementary material at http://dx.doi.org/10.1063/1.4923422 for RKR potential energy curve and its interpolation/extrapolation by LEVEL, *ab initio* potential and DMF, line list including positions and intensities, $A_{v'v}$ and $f_{v'v}$ values, and PGOPHER input file.